NASA Technical Memorandum 104382

Destructive Physical Analysis Results of Ni/H_2 Cells Cycled in LEO Regime

Hong S. Lim and Gabriela R. Zelter
Hughes Aircraft Company
Torrance, California

John J. Smithrick
Lewis Research Center
Cleveland, Ohio

and

Stephen W. Hall
Naval Weapons Support Center
Crane, Indiana

Prepared for the
26th Intersociety Energy Conversion Engineering Conference
sponsored by ANS, SAE, ACS, AIAA, ASME, IEEE, and AIChE
Boston, Massachusetts, August 4-9, 1991

NASA

DESTRUCTIVE PHYSICAL ANALYSIS RESULTS OF NI/H_2 CELLS CYCLED IN LEO REGIME

Hong. S. Lim and Gabriela R. Zelter
Hughes Aircraft Company
Torrance, California

John J. Smithrick
National Aeronautics and Space Administration
Lewis Research Center
Cleveland, Ohio

and

Stephen W. Hall
Naval Weapons Support Center
Crane, Indiana

ABSTRACT

Six 48-Ah individual pressure vessel (IPV) Ni/H_2 cells containing 26 and 31 percent KOH electrolyte have been on a low earth orbit (LEO) cycle life test. All three cells containing 31 percent KOH have failed (3729, 4165, and 11 355 cycles) while those with 26 percent KOH have been cycled for over 14 000 cycles in the continuing test. We have carried out post-cycle characterization tests and destructive physical analyses (DPA) of the three failed cells. The DPA included visual inspections, measurements of electrode thickness, scanning electron microscopy, chemical analyses, and measurements of nickel electrode capacity in an electrolyte flooded cell. The cycling failure was due to decrease of nickel electrode capacity. As possible causes of the capacity decrease, we have observed electrode expansion, rupture and corrosion of the nickel electrode substrate, active material redistribution, and accumulation of electrochemically undischargeable active material with cycling.

INTRODUCTION

A dramatic improvement of cycle life of a Ni/H_2 cell has been demonstrated in boilerplate test cells [1,2] by using 26 percent KOH electrolyte instead of conventional 31 percent. To confirm this improvement NASA Lewis Research Center has a contract with the Naval Weapons Support Center (NWSC) to test six 48-Ah Hughes recirculation design IPV Ni/H_2 flight cells [3]. Three of these cells contain 26 percent KOH electrolyte and three contain 31 percent KOH.

The cells are being tested under a low earth orbit [LEO] regime consisting of a 54-min charge followed by a 36-min discharge at 80 percent depth of discharge and 10 °C. All three cells containing 31 percent KOH electrolyte have failed after 3729, 4165, and 11 355 cycles, by low end-of-discharge voltage (≤1.0 V) while the other three cells containing 26 percent KOH electrolyte have been cycled over 14 000 cycles without a cell failure. The present report describes results of post-cycle characterization tests and destructive physical analyses (DPA) on the three failed and discusses possible cause of the failure.

EXPERIMENTAL

Cell Design

All cells were flight quality cells which were rated at 48 Ah and equipped with individual strain gauges. Cell stacks were made of 44 nickel electrodes in a recirculation stack design using zirconia separators. All cells had a nickel electrode precharge. Three of six cells were activated using 31 percent KOH electrolyte. The other three cells were activated using 26 percent KOH electrolyte.

Post-Cycle Characterization

Post-cycle characterization tests at NWSC included measurements of cell capacity by discharging cells at 24 A (C/2), 48 A (C), 67.2 A (1.4C) and 96 A (2C), respectively, to 1.0 V after charging them at 24 A for 2 hr and then additional charging at 4.8 A (C/10 rate) for 6 hr at 10 °C. Cell internal resistance was determined from the slopes of mid-discharge voltages versus discharge rates.

Pre-disassembly test at Hughes included additional capacity measurements in addition to a cell leak test, cell pressure measurement by strain gauge, and visual inspections. First cycle (conditioning cycle) involved charging cells at 4.8 A (C/10 rate) for 18 hr followed by discharging them at 67.2 A (1.4C) to 1.0 V and further discharge at 4.8 A to 0.0 V at 10 °C. Second and third cycles (also at 10 °C) involved charging cells at 24 A for 2 hr and then additional charging at 4.8 A for 6 hr followed by discharging them at 67.2 A (1.4C) to 1.0 V and further discharge at 4.8 A to 0.0 V. The fourth cycle test was a 72-hr open-circuit stand test at 20 °C after charging cells at 4.8 A for 10 hr.

Disassembly Analyses

All cells were shorted using a 1-Ω (5 W) resistor for a minimum of 16 hr followed by a dead short for a minimum of 4 hr prior

to the disassembly. Disassembly analyses included visual inspections and photographing of the cell stacks and components, inspection of "popping" damage of hydrogen electrodes, electrolyte analyses for KOH and carbonate after a Soxhlet extraction of a portion of the stack (five unit cells), electrode thickness measurements, flooded electrolyte capacity measurements of nickel electrodes with three different amount of overcharge, chemical analyses of nickel electrodes, and scanning electron microscopy (SEM).

Flooded electrolyte capacity measurements were carried out in a 31 percent KOH electrolyte. Each cell consisted of a pair of nickel electrodes from near top, middle, and bottom of the original cell stack position. Three duplicate measurements were carried out after charging cells at 0.22 A for 16 hr followed by discharging them at 1.10 A to -1.5 V versus a nickel sheet counter electrode.

RESULTS OF PRE-DISASSEMBLY CHARACTERIZATIONS

Charge voltage curves C/2 rate before and after the cycle life test are shown in figure 1 for cell 3 to illustrate characteristic voltage changes. The charge voltage was increased by 30 to 40 mV after the cycle life test. Typical cell voltages at various discharge rates before and after the cycle life test are shown in figure 2. All three cells showed lower discharge voltages after the cycle life test than before the test. The depression in discharge voltage with cycle life test was attributed to formation of γ-phase NiOOH as the electrode is cycled in relatively high concentration (31 percent) of KOH [4]. The effect of discharge rates on the voltage of cycled cell 2 is shown in figure 3. All cells showed faster voltage decrease as the discharge rate was increased after the cycle life test than before the test. Plots of mid-discharge voltage versus discharge current gave good straight lines indicating that the voltage drop was ohmic. Cell internal resistance values determined from the slopes of these plots are summarized in table I. The data show that the internal resistance of the cells are increased by 12 to 47 percent after the cycle life test.

Capacity values at the beginning of life (BOL) and the end of life (EOL) are shown against discharge rates in figure 4. Both values of capacity before and after the cycle life test decrease as the discharge rates increase. However, the decrease of capacity after the cycle test (EOL) is more pronounced than before the cycle test (BOL). Similar observations were also reported earlier from boilerplate cells testing [2,5]. Capacities measured at 1.4 C rate to 1 V and residual capacities at C/10 rate to 0 V before and after the cycle life test are shown in figure 5. The capacities to 1 V decreased by 24.3, 29.0, and 31.1 percent for cells 1 to 3, respectively. The residual capacities increased drastically, but the overall capacities decreased by 10 to 14 percent. Figure 6 shows cell charge retention values at BOL and EOL after a 10-hr charge at 4.8 A followed by a 72-hr open circuit at 20 °C. The charge retention values are substantially decreased with cycling. This decrease may be due to a combination of reduction in charging efficiency and increase of self-discharge rate.

RESULTS OF DISASSEMBLY ANALYSES

All three cells showed no indication of leak or damage of cell case prior to the disassembly. Strain gauge readings immediately prior to the disassembly of cells 1 to 3 indicated cell pressure of 63, 71, and 122 psig, respectively. These pressure values indicate that the net increase of the pressure correspond to 167, 175 and 226 psi, respectively, from the initial nickel precharge condition which corresponds to a -104 psig of H_2. These values agree with the increase in end-of-charge pressure (EOCP) during cycling within an experimental error. This pressure increase is believed to be due to corrosion of nickel sinter substrate (2) during the cycling test.

Visual Inspections

All cell stacks looked dry without any excess electrolyte outside the stack. The stack of cell 3 cell looked drier than the others. All stacks were free of visible damage. Nickel electrodes from cells 1 and 2 showed only minor degree of gas screen imprints on the side which faced the screen indicating that there was only light extrusion of active material. The degree of extrusion appears to be relatively light for the number of cycles (3729 and 4165). The electrodes from cell 3 (11 355 cycles) showed clear imprints of gas screen indicating that there was extrusion of active material out of the sinter substrate although it did not appear to be excessive in comparison with those observed earlier with a comparable number of cycles [5]. When zirconia separators were peeled off the nickel electrodes from cells 1 and 2, the separators looked grey, while those from cell 3 were black indicating that extrusion of active material was more pronounced with cell 3. There was no loose black powder on the inside wall of the pressure vessel. There was indication of localized hydrogen-oxygen recombination (popping) on the hydrogen electrodes which is commonly observed from cycled cells of a similar design. Visible variations of the popping from one cell to another were rather minimal. In summary, there were no apparent visible signs that caused the failure.

Electrode Thickness Change

Electrode thickness were measured at three different locations on each electrode using a micrometer. Individual electrode expansion data at various electrode positions in the stack are summarized in table II. Average thickness of electrodes from cells 1 to 3 were 0.0343 (19 percent expansion from initial 0.0289), 0.0351 (22 percent expansion from initial 0.0288), 0.040 (37 percent expansion from initial 0.0291) in., respectively. However, we did not identify a definite correlation between the degree of expansion and the electrode position in the stack. The average value of electrode expansion is shown against number of cycles in figure 7.

Scanning Electron Micrography (SEM)

SEM pictures of various magnifications (100 to 500X) of electrode surface, fractured surface, metallographic cross-sections of nickel electrodes were studied. We could not identify any characteristic changes with the cycling in the pictures of the electrode and fractured surfaces. Pictures of the cross-sectional area showed dimensional expansion, active material extrusion, and damages of sinter by the expansion as shown in figure 8. These changes are similar to those reported earlier [2,5].

Chemical Analyses

Results of electrolyte analysis showed that total potassium ion concentration was 30 percent as KOH for cell 2 and 32.6 percent for cell 3. Concentration of K_2CO_3 was 1.3 percent as KOH for

cell 2 and 2.0 percent for cell 3. Higher concentrations of total potassium ion and K_2CO_3 for cell 3 than those for cell 2 are consistent with an increased corrosion of nickel substrate [2] for cell 3 due to its longer cycling time.

The compositions of active mass (active material and metallic nickel) are shown against the number of cycles in figure 9. Total amount of ionic Ni and Co (active material) increased with cycling while the amount of metallic nickel decreased. These changes are due to corrosion of the nickel metal. In agreement with this result, we had also observed similar corrosion of the electrode substrate material earlier [2]. Decrease of the cobalt concentration in the active material with cycling as shown in Fig. 10 is also consistent with the nickel corrosion to produce additional nickel oxide/hydroxide in the active material.

The amount of ionic Ni and Co in oxidation state (III) (abbreviated as Ni(III)) increased noticeably as the electrodes are cycled as shown in figure. 11. This result indicates that the electrodes are becoming increasingly more difficult to discharge completely as they are cycled as observed earlier [5].

Changes in Electrode Capacity

Figure 12 shows capacity values in a flooded cell of 31 percent KOH electrolyte of a new nickel electrode and those from the cycled cells. The individual data column represent an average value of two measurements on a pair of electrodes after C/10 rate charging for 16 hr. The average capacity reductions (from the new ones) of the electrodes from each cycled cell range from 29 to 37 percent, while the capacity decreases in the Ni/H_2 cells were 24 to 31 percent (fig. 5). However, the individual electrode capacities were considerably more variable as shown in figure 12, especially, for cells 1 and 2. Another noticeable observation was that the discharge voltages of the electrodes which had heavy capacity loss were lower than others.

DISCUSSIONS

Cycle test results show that all three cells failed due to a cell capacity decrease with cycling. No apparent physical anomalies including an indication of "soft short" were identified during disassembly. Even though cell stacks, especially, that of cell 3, were relatively dry, the cell failure by electrolyte dry-out as the direct cause of the failure appears to be unlikely, because the amount of nickel electrode capacity decrease in the electrolyte flooded cell was comparable with that of the starved cell capacity. SEM pictures show rupture of sinter structure, especially for the electrodes from cell 3. Chemical analysis results indicated that there was a measurable amount of nickel metal corrosion. But these sinter damages and corrosion alone do not appear to be the direct cause of the electrode capacity decrease either, because some of the electrodes from cells 1 and 2 showed more capacity decrease than those from the cell 3 which showed more severe sinter damage. Even though the nickel electrode expansion was substantial (37 percent for cell 3), there was no mechanical damage in the cell that would cause a failure or an excessive capacity decrease by the expansion. The cause of the capacity decrease might possibly be a combination of the electrode expansion, rupture and corrosion of the nickel electrode substrate, and active material redistribution, leading to accumulation of an electrochemically undischargeable active material.

Cells 1 and 2 failed much earlier in cycling than cell 3. The average decrease in the nickel electrode capacity in cells 1 and 2 in 3729 and 4165 cycles, respectively, were comparable with that in cell 3 in 11 355 cycles. But the electrode capacity in cells 1 and 2 were extremely uneven with one out of three electrode pairs showing unusually low capacity (fig. 12). These low capacity electrodes appeared to be mainly responsible for the failure of both cells. However, what caused the unusual low capacity of these electrodes is not clear from the present DPA results. Neither electrodes showed an excessive expansion (table IV) to account for the severe capacity loss nor showed deficiency of active material by chemical analysis to account for the low capacity. Nevertheless, the amount of electrochemically undischargeable active material (fig. 11) was roughly proportional to the number of cycles indicating that the accumulation of this material is one of the failure mechanisms.

We are planning to carry out DPA study of the remaining three cells containing 26 percent KOH electrolyte when they fail. A further elucidation of the failure mechanism might be possible after completion of this study.

CONCLUDING REMARKS

All three cells failed in cycling due to capacity decrease of the nickel electrodes as evidenced by capacity values in flooded electrolyte cells. As possible causes of the capacity decrease, we have observed electrode expansion, rupture and corrosion of the nickel electrode substrate, active material redistribution, and accumulation of electrochemically undischargeable active material with cycling. Cell 3 appeared to be failed by a gradual wear-out by these changes. Some of the electrodes from cell 1 and cell 2 have shown a premature capacity fading which was responsible for an early failure of these cells. However, chemical analysis of the electrodes which showed the premature capacity fading did not give any anomalous results. The mechanism of this premature capacity fading is not clearly understood by the present DPA. No cells showed any apparent superficial mechanical damage (eg., shorts) which can be attributed to cell failure. All cells showed some increase in internal resistance after the cycle test but this increase itself does not appear to be the direct cause of failure. All cells showed increase in charge voltage, and decrease in discharge voltage after the cycle test.

ACKNOWLEDGMENTS

This work is supported by a NASA Lewis Research Center (Contract No. NAS 3-22238). Authors would like to thank Mr. D.B. Losee of Hughes Aircraft Company for pre-disassembly capacity measurements.

REFERENCES

[1] H.S. Lim and S.A. Verzwyvelt, "KOH concentration effect on the cycle life of nickel-hydrogen cells. III. Cycle life test," J. Power Sources, vol. 22, Mar.-Apr. 1988, pp. 213-220.

[2] H.S. Lim and S.A. Verzwyvelt, "KOH concentration effect on the cycle life of nickel-hydrogen cells. IV. Results of failure analyses," J. Power Sources, vol. 29, Feb. 1990, pp. 503-519.

[3] J.J. Smithrick and S.W. Hall, "Effect of KOH concentration on LEO cycle life of IPV nickel-hydrogen flight battery cells," Twenty-Five Years of Progress and Future Prospects (25th IECEC), vol. 3, AIChE, New York, 1990, pp. 16-21.

[4] H.S. Lim and S.A. Verzwyvelt, "Electrochemical Behavior of Heavily Cycled Nickel Electrodes in Ni/H2 Cells Containing Electrolytes of Various KOH Concentrations," Proceedings, Symposium on Nickel Hydroxide Electrodes, Electrochemical Society Proceedings, vol. 90-4, Electrochemical Society, 1990, pp. 341-355.

[5] H.S. Lim and S.A. Verzwyvelt, "Long life nickel electrodes for a nickel-hydrogen cell: Results of an accelerated test and failure analyses," Advanced Energy Systems—Their Role in Our Future (19th IECEC), vol. 1, American Nuclear Society, 1984, pp. 312-318.

TABLE I. - SUMMARY OF CELL INTERNAL RESISTANCE DATA FROM MID-DISCHARGE VOLTAGES

Cell	Before life test, mΩ	After life test, mΩ	Change, percent
1	1.1	1.3	18
2	1.26	1.41	12
3	1.06	1.56	47

TABLE II. - POSITIVE PLATE THICKNESS OF CELLS 1 TO 3. (THE POSITIVE TERMINAL WAS AT THE TOP END OF THE STACK.)

Electrode position in stack	Electrode expansion, percent		
	Cell 1	Cell 2	Cell 3
1 (top of stack)	——	18.5	31.7
4	18.9	——	——
11	——	16.9	——
12	——	17.5	35.9
13	21.5	——	38.5
18	14.5	16.9	42.9
19	17.6	23.1	39.5
27	19.8	23.1	37.6
28	20.2	23.3	43.8
36	20.3	26.8	31.2
37	14.6	——	36.8
39	21.5	26.9	36.2
44 (bottom of stack)	17.0	26.2	——
Av	18.6	21.9	37.4
Std dev	2.57	4.12	4.1

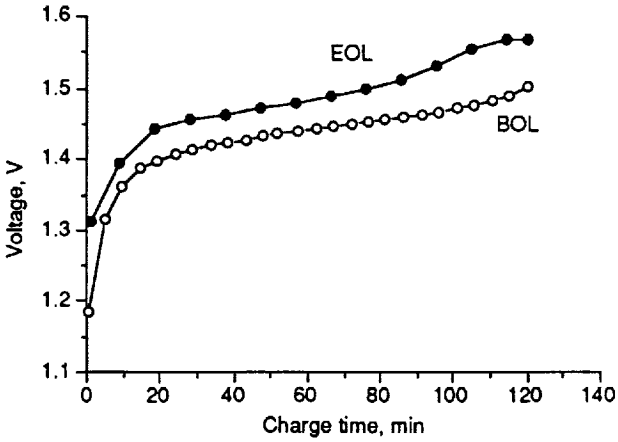

Figure 1.—Charge voltage-time curves of cell 3 at C/2 rate before (BOL) and after (EOL) the cycle life test.

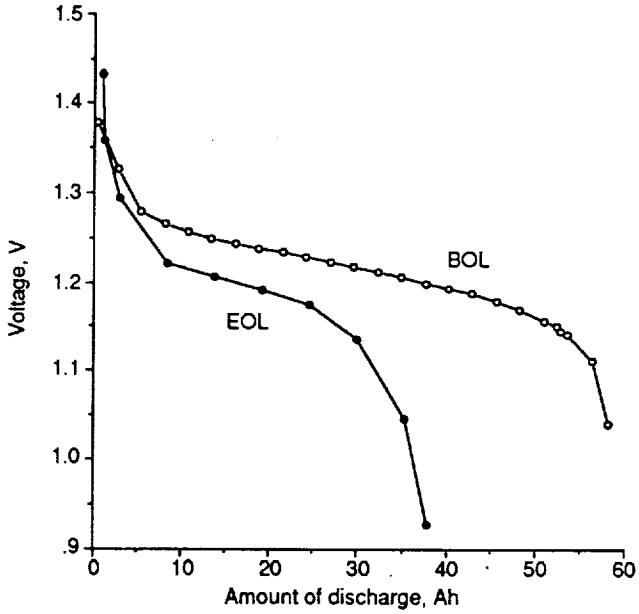

Figure 2.—Voltages vs. amount of discharge at 1.4 C discharge rate before and after the cycle life test for cell 3.

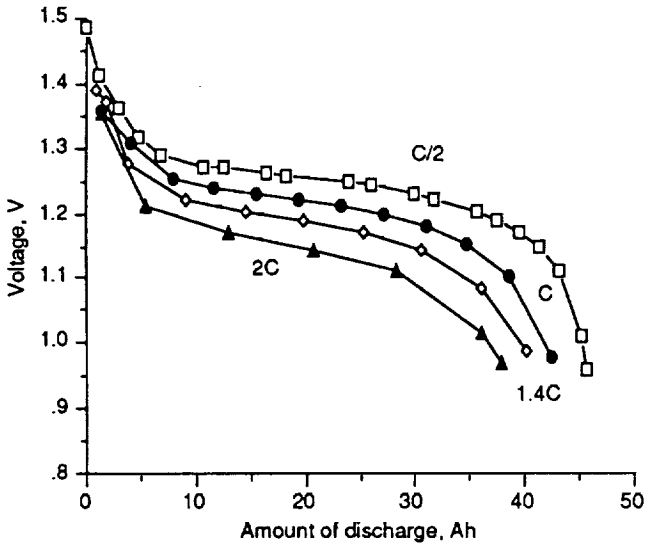

Figure 3.—Typical voltage curves vs. amount of discharge at various discharge rates after the cycle life test for cell 2.

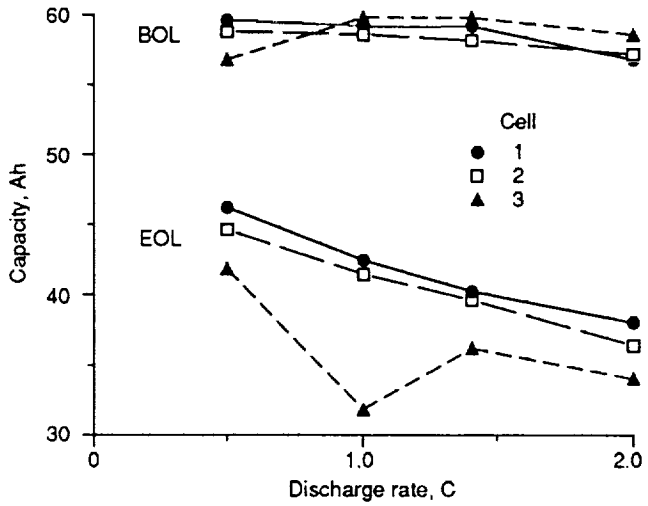

Figure 4.—Cell capacities vs. discharge rates before (BOL) and after (EOL) the cycle life test.

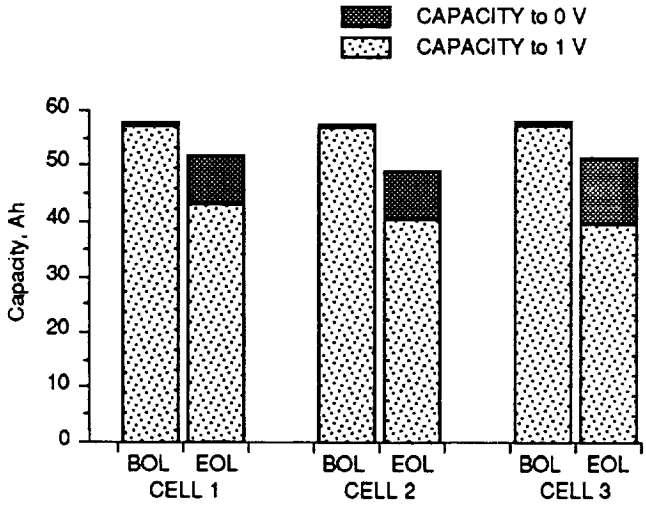

Figure 5.—Cell capacity measured at 1.4 C rate discharge to 1.0 V and then C/10 rate discharge to 0.0 V.

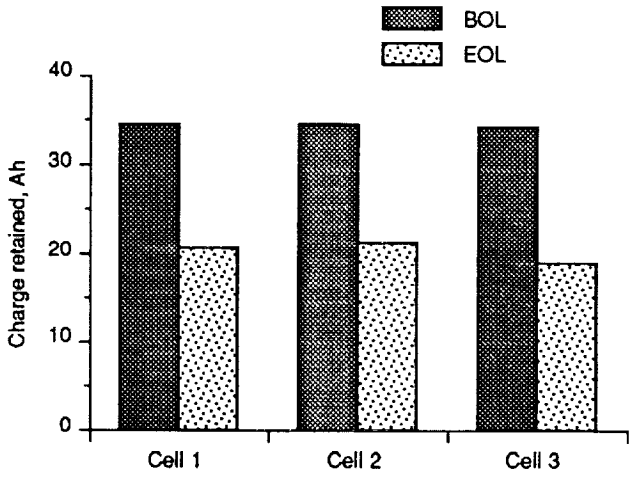

Figure 6.—Charge retention after 72-hr open circuit stand at 20 °C after charging for 10 hr at 4.8 A.

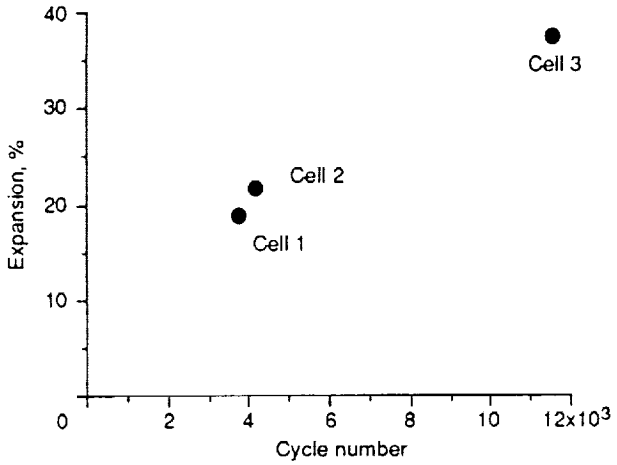

Figure 7.—Average expansion of nickel electrodes vs. number of cycles. Data points represent and average value from each cell.

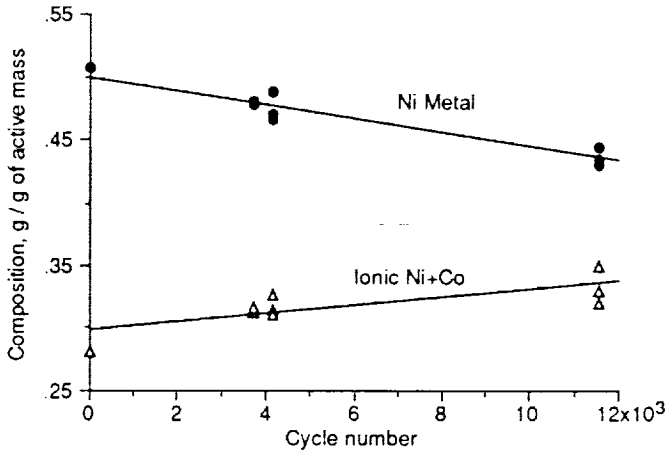

Figure 9.—Amount of ionic Ni and Co and amount of metallic nickel in the active mass are shown against the number of cycles. Individual data points represent average measured values for each pair of the electrodes used for the flooded cell capacity measurements.

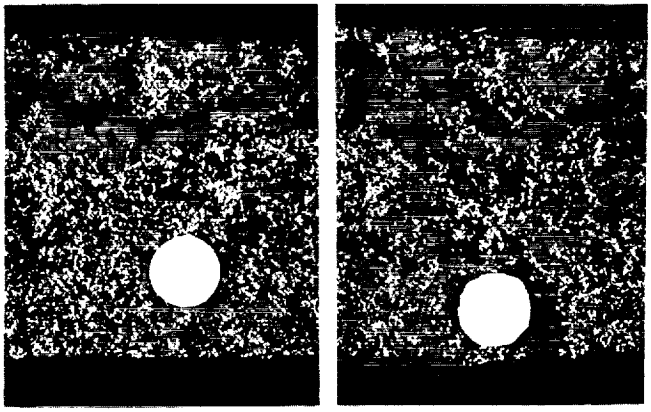

(a) Cell 1. (b) Cell 2.

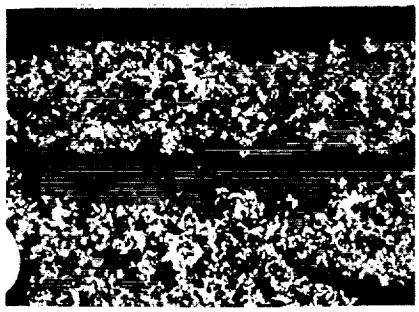

(c) Cell 3.

Figure 8.—SEM pictures (approximately 75X) of the cross-sectional area of nickel electrodes from (a) cell 1, (b) cell 2, and (c) cell 3.

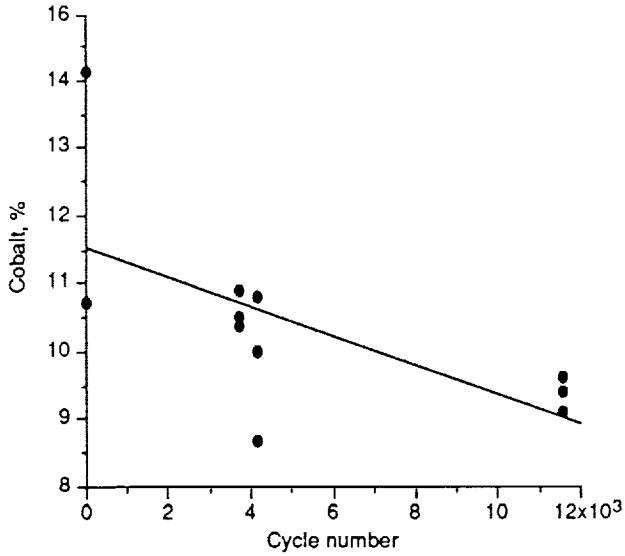

Figure 10.—Co content in the active material against the number of cycles. (See comments for Fig. 9)

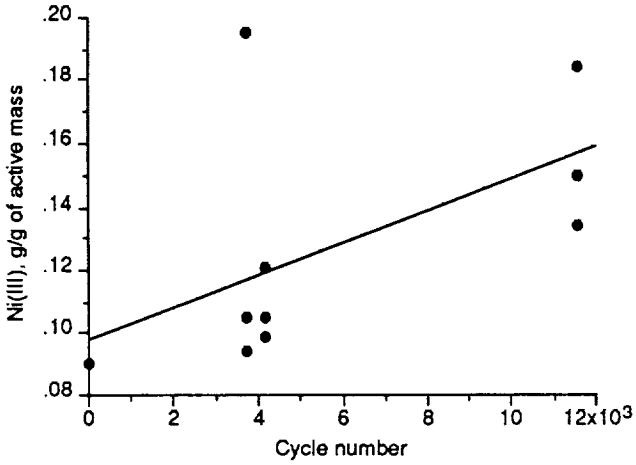

Figure 11.—Amount of ionic Ni and Co in oxidation state (III) (abbreviated at Ni(III)) in the active mass against the number of cycles. (See comments for Fig. 9.)

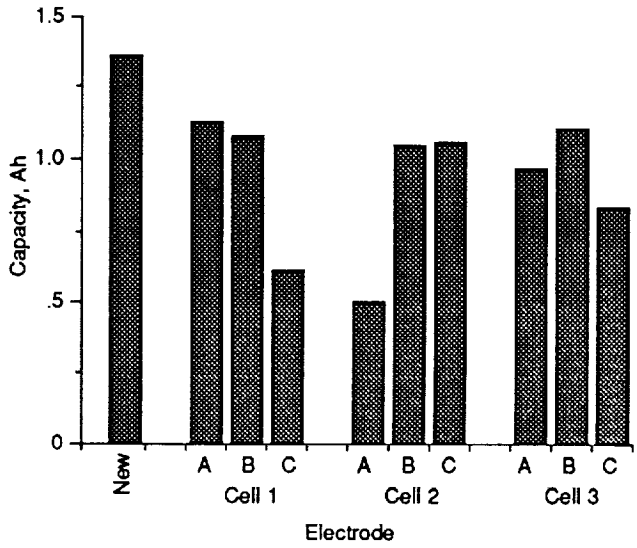

Figure 12.—Nickel electrode capacity values in a flooded electrolyte cell.

NASA
National Aeronautics and Space Administration

Report Documentation Page

1. Report No.	2. Government Accession No.	3. Recipient's Catalog No.
NASA TM -104382		

4. Title and Subtitle
Destructive Physical Analysis Results of Ni/H_2 Cells Cycled in LEO Regime

5. Report Date

6. Performing Organization Code

7. Author(s)
Hong S. Lim, Gabriela R. Zelter, John J. Smithrick and Stephen W. Hall

8. Performing Organization Report No.
E -6191

10. Work Unit No.
506-41-21

9. Performing Organization Name and Address
National Aeronautics and Space Administration
Lewis Research Center
Cleveland, Ohio 44135 - 3191

11. Contract or Grant No.

13. Type of Report and Period Covered
Technical Memorandum

12. Sponsoring Agency Name and Address
National Aeronautics and Space Administration
Washington, D.C. 20546 - 0001

14. Sponsoring Agency Code

15. Supplementary Notes
Prepared for the 26th Intersociety Energy Conversion Engineering Conference sponsored by ANS, SAE, ACS, AIAA, ASME, IEEE, and AIChE, Boston, Massachusetts, August 4-9, 1991. Hong S. Lim and Gabriela R. Zelter, Hughes Aircraft Company, Torrance, California; John J. Smithrick, NASA Lewis Research Center; Stephen W. Hall, Naval Weapon Support Center, Crane, Indiana. Responsible person, John J. Smithrick, (216) 433-5255.

16. Abstract
Six 48-Ah individual pressure vessel (IPV) Ni/H_2 cells containing 26 and 31 percent KOH electrolyte have been on a low earth orbit (LEO) cycle life test. All three cells containing 31 percent KOH have failed (3729, 4165, and 11,355 cycles) while those with 26 percent KOH have been cycled for over 14,000 cycles in the continuing test. We have carried out post-cycle characterization tests and destructive physical analyses (DPA) of the three failed cells. The DPA included visual inspections, measurements of electrode thickness, scanning electron microscopy, chemical analyses, and measurements of nickel electrode capacity in an electrolyte flooded cell. The cycling failure was due to decrease of nickel electrode capacity. As possible causes of the capacity decrease, we have observed electrode expansion, rupture and corrosion of the nickel electrode substrate, active material redistribution, and accumulation of electrochemically undischargeable active material with cycling.

17. Key Words (Suggested by Author(s))	18. Distribution Statement
Nickel hydrogen batteries Failure analysis Alkaline batteries Storage batteries	Unclassified - Unlimited Subject Category 20

19. Security Classif. (of the report)	20. Security Classif. (of this page)	21. No. of pages	22. Price*
Unclassified	Unclassified	8	A02

NASA FORM 1626 OCT 86

*For sale by the National Technical Information Service, Springfield, Virginia 22161